



Contents lists available at ScienceDirect

CIRP Annals - Manufacturing Technology

journal homepage: <http://ees.elsevier.com/cirp/default.asp>

Subsurface damage in milling of lightweight open-cell aluminium foams

Haipeng Qiao^a, Saurabh Basu^b, Christopher Saldana^a, Soundar Kumara (1)^{b,*}^aGeorge W. Woodruff School of Mechanical Engineering, Georgia Institute of Technology, Atlanta, GA 30332, USA^bHarold and Inge Marcus Department of Industrial and Manufacturing Engineering, The Pennsylvania State University, University Park, PA 16801, USA

ARTICLE INFO

Keywords:
Surface integrity
Machining
3D image processing

ABSTRACT

The present study examined the surface integrity of open cell aluminium foams at full volume using X-ray micro-computed tomography. The structural network was reconstructed in voxel models, for which watershed segmentation and medial axis extraction was utilized to identify interconnected pore (air) and strut (solid) phases. From these models, post-mortem surface integrity characteristics, including pore size, strut bending angle and preferential strut orientation were characterized as a function of controllable parameters of cutting speed, feed rate and depth of cut. Post-mortem characterization of the damage enabled mapping of fundamental failure mechanisms in the mechanics of the subsurface deformation.

© 2017 Published by Elsevier Ltd on behalf of CIRP.

1. Introduction

Metallic foams and other low density lattice materials have found application in biomedical components due to their attractive physical and mechanical properties, including low weight, high specific stiffness, high strength, high corrosion resistance, increased permeability and enhanced biocompatibility properties [1–4]. Open cell foams are well suited for these applications because their interconnected porous structure supports migration and proliferation of cells by mass transport, promotion of implant vascularization and mitigation of stress shielding for surrounding hard tissue [1,5]. Overall functionality of these porous implant materials is dependent on the morphology of the pore-strut network. In this regard, surface integrity in terms of surface/subsurface foam structure are critical quality factors due to their deterministic effects on biointegration performance. It has been reported that damage to cell morphology can disrupt the transport capability of the otherwise highly interconnected porous network, thereby limiting bone ingrowth and reducing biomechanical integrity of the implantation [1,5].

Among processing methods capable of shaping final implant geometry from billet-type porous materials, cutting based methods are of strong interest for processing of hard foams, as these may provide for more direct compatibility with machining-based finishing processes used in the manufacture of high volume structural implants, including multi-axis milling and Swiss style turning [6,7]. However, use of cutting-based processing methods for these complex materials requires a detailed understanding of the damage occurring during surface generation in porous metal foams and the corresponding effects on surface integrity and implant performance.

Deformation and failure mechanisms and the mechanics of processing of hard foams are far from well understood and remain

the subject of interest for experimental and modelling investigations. Several experimental studies have been made to explore the effect of machining parameters on metallic foam response [8–13]. For instance, Schoop et al. [10] utilized scanning electron microscopy (SEM)-based characterization to assess surface morphology changes with application of cryogenic cooling to machining of porous tungsten. Bram et al. [11] also utilized SEM-based observations to compare cutting and grinding approaches and their effects on subsurface damage in finishing of titanium foams. Deglurkar et al. [12] expanded these observations and made histological measurements with optical microscopy of incremental sections of machined porous tantalum implants. While these investigations have contributed to understanding processing effects for these porous materials, prior measurements have been limited to 2D analyses instead of full volume measurements of surface integrity.

Development of X-ray-based micro-computed tomography (CT) as a technique for measurement of complex 3D structure provides an attractive route for assessing manufacturing-induced effects on morphological structure of hard foams. CT relies on measurement of local X-ray attenuation to generate high resolution 3D maps of internal structure. In terms of its metrological application, several works have sought to identify the role of controllable CT measurement variables (e.g., voltage, current, thresholding algorithm, etc.) in determining overall measurement uncertainty [14–16]. In its application for studying structure of hard foams, prior attention has focused on use of CT to establish mechanics of damage and failure of foams in generalized static loading, including in quasi-static tension and compression [17–19]. These studies have elucidated various plastic failure phenomena, including localized plastic accommodation in deformation bands and plastic hinging mechanisms in individual foam struts. This has been supported by construction of 3D displacement maps from image pairs using digital volume correlation methods [19,20].

In contrast to uniaxial loading, the thermomechanical response in machining of porous foams is substantially more complex due to

* Corresponding author.

E-mail address: skumara@psu.edu (S. Kumara).

the intrinsic macroscale heterogeneity present during deformation which gives rise to various types of damage including smearing, fracture and cell dilation [8–12,21]. Full volume measurements of surface damage in machined foams are important in developing high fidelity understanding of machining-induced effects on foam structure and have yet to be established. To address the need, the present study seeks to directly measure the effect of machining parameters on surface and subsurface structure of hard metal foams using CT-based characterization. Damage in terms of morphological changes to the pore-strut network is evaluated in context of the machining parameters selected.

2. Experiment

A milling operation on open cell Al foams was carried out using a face mill having a diameter of 50 mm with two square Fansteel SEC-422/2A5 uncoated carbide inserts (rake angle 6°). The workpieces were open cell AA6061T6 foams in the form of $90 \text{ mm} \times 40 \text{ mm} \times 13 \text{ mm}$ rectangular blocks. Specimens were produced using wire electrical discharge machining to limit damage to the work surface. A Proto Trak K3 SMX milling machine was used at cutting speeds of $v_c = \{2.6, 3.7, 5.2 \text{ m/s}\}$, linear feed rates of $v_f = \{0.051, 0.102, 0.204 \text{ mm/min}\}$, and axial depths of cut $a_p = \{1.0, 1.5, 2.0 \text{ mm}\}$. Clamping forces applied to the workpieces were minimal so to limit damage caused by workholding. This was verified from CT of the test specimens. The experimental conditions are summarized in Table 1 and the machining configuration is depicted in Fig. 1, where ND, TD and FD represent the normal, transverse and feed directions, respectively. A micro-CT platform (Zeiss Metrotom) was used to characterize the workpieces before and after machining with a spatial resolution of $57.32 \mu\text{m}/\text{voxel}$. The X-ray tube was used at 80 kV and $100 \mu\text{A}$, this corresponding to an $8 \mu\text{m}$ focal spot size. The samples were rotated incrementally with a step of 0.25° over an angular range of 360° as 2D projections were acquired with a $1536 \text{ px} \times 1900 \text{ px}$ sensor. A Feldkamp-type cone-beam reconstruction algorithm was used for reconstruction.

Table 1
Experimental conditions (L=low, M=medium, H=high).

	1	2	3	4	5	6	7	8	9	10	11	12	13	14	15
v_c	L	L	L	L	L	L	L	L	L	M	M	M	H	H	H
v_f	L	L	L	M	M	M	H	H	H	L	L	L	L	L	L
a_p	L	M	H	L	M	H	L	M	H	L	M	H	L	M	H

A MATLAB code was implemented to render and characterize the 3D foam structure. First, a binarization process was implemented to classify each voxel as either solid or empty space by setting a global grey level threshold due to the high contrast between the air and solid phases, as shown in the histogram of Fig. 1. An ISO50 threshold setting approach was applied, wherein the threshold was given by the average of the median values for the air phase and solid phase peaks. Voxels with intensity above this threshold were identified as solid phase and those below as air phase. To analyze the individual pores, a watershed-based analysis was used to isolate and encode

each voxel according to individual pores. The algorithm assigned each pore a unique label based on a 3D distance map in which each voxel centre had a value of the distance to the nearest solid-phase voxel and each pore centroid was located at a relative peak in the distance map. To analyze the solid network, medial axis extraction was conducted to isolate the solid phases (i.e., struts). This provided determination of length and local curvature information of each strut segment. A volumetric registration algorithm was used to align the two datasets.

3. Results and discussion

The effects of milling process parameters on the surface structure of the foam samples are measurable in terms of structural changes to solid strut configurations and the resulting pore morphology. Fig. 2(a) provides a graphical depiction of voxel models of both initial and post-machined samples under $v_c = 2.6 \text{ m/s}$, $v_f = 0.204 \text{ mm/min}$, $a_p = 1.5 \text{ mm}$, at subsurface depths of $d = 1.5 \text{ mm}$ (i and ii) and $d = 8.5 \text{ mm}$ (iii and iv). Evidence of strut bending and fracture can be observed at the smaller subsurface depth, compared to a relatively unchanged/undistorted strut configuration deeper into the workpiece surface. The CT-measured voxel model was processed using the MATLAB-based analysis and the results of the pore segmentation and medial axis extraction are shown in Fig. 2. In terms of effects on the pore-phase network, Fig. 2(b) shows that close to the machined surface, the initial pore (i) was divided into sub-pores (ii) due to volume changes associated with local strut bending, causing multiple local distance maxima to form in the 3D distance map. In comparison, far from the machined surface, the lack of distortion in the solid strut network resulted in a virtually equivalent pore morphology. To assess morphological changes to the solid-phase strut network, Fig. 2(c) shows the medial axis extraction results for the voxel model of Fig. 2(a). In the vicinity of the machined surface, formation of new strut branches occurred with greater frequency, likely caused by strut fracture within the deformation zone. From these structural measurements, changes in total strut surface area and local strut curvature were measured to quantify deformation-induced effects.

To determine the effects of machining parameters on surface integrity, the effective pore size was characterized as a function of subsurface depth. In this regard, the location of each pore in the workpiece was characterized according to the position of its centroid, occurring at the relative maximum in the local distance map. The equivalent pore diameter was determined by the assumption that each pore can be modelled as an ideal sphere, where the pore volume is given by the sum of all voxels associated with a specified pore label in the watershed segmentation. Fig. 3 shows a representative plot to assess the effective pore size as a function of subsurface depth for the machining condition of $v_c = 2.60 \text{ m/s}$, $v_f = 0.051 \text{ mm/min}$, $a_p = 1.5 \text{ mm}$. From the figure, the initial foam structure had a roughly constant equivalent pore diameter of 2.2 mm throughout the part volume. Representative pore morphologies are provided in the inset of Fig. 3 at locations A and B in the subsurface depth, indicating a roughly spherical

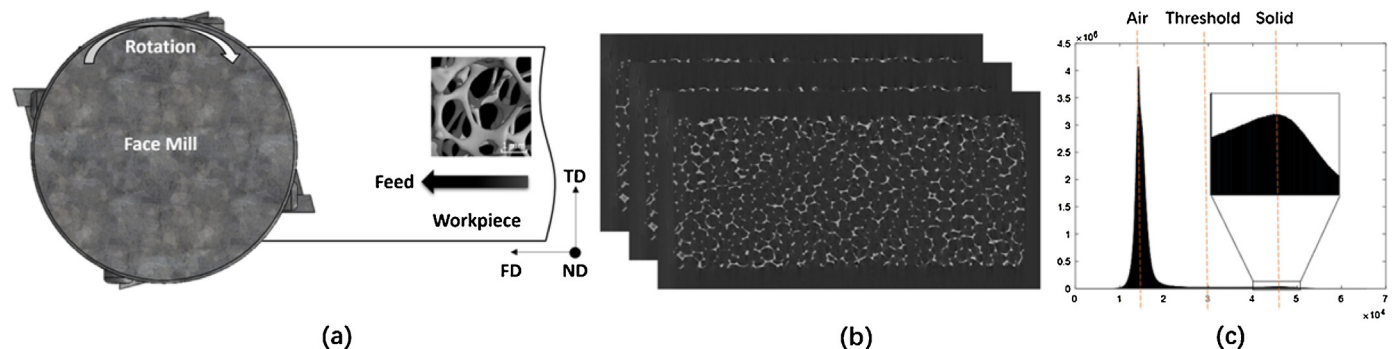


Fig. 1. (a) Experimental configuration and (b) representative reconstructed image slices, and (c) grayscale intensity histogram of 3D reconstructed volume, with air phase (median), solid phase (median) and ISO 50 threshold value marked using dash lines.

Download English Version:

<https://daneshyari.com/en/article/5466952>

Download Persian Version:

<https://daneshyari.com/article/5466952>

[Daneshyari.com](https://daneshyari.com)